Frontiers in Optics + Laser Science 2023 (FiO/LS) © Optica Publishing Group 2023

Integrated Polarization-Diverse Grating Emitters for Trapped-Ion Quantum Systems

Sabrina Corsetti[1], Ashton Hattori[1], Reuel Swint[2], Milica Notaros[1], Gavin N. West[1], Tal Sneh[1], Felix Knollmann[1], Patrick T. Callahan[2], Thomas Mahony[2], Ethan R. Clements[1], Dave Kharas[2], Cheryl Sorace-Agaskar[2], Robert McConnell[2], John Chiaverini[1,2], and Jelena Notaros[1,†]

[1]Research Laboratory of Electronics, Massachusetts Institute of Technology, Cambridge, MA 02139, USA
[2]Lincoln Laboratory, Massachusetts Institute of Technology, Lexington, MA 02421, USA
[†]notaros@mit.edu

Abstract: We design and experimentally demonstrate the first pair of integrated TE- and TM-emitting gratings at a wavelength of 422nm, targeting the $5^2S_{1/2}$-$5^2P_{1/2}$ transition of $^{88}Sr^+$ ions, to enable operations requiring diverse polarizations for integrated-photonics-based trapped-ion quantum systems.

1. Introduction

Systems of trapped ions are a promising modality for quantum information processing due to their long coherence times and strong ion-ion interactions, which enable high-fidelity two-qubit gates [1]. Most current implementations are comprised of complex free-space optical systems, whose large size and susceptibility to vibrations and drift can limit the fidelity and addressability of ion arrays, hindering scaling to large numbers of qubits. Recently, integrated-photonics-based devices and systems have been demonstrated as an avenue to address these challenges [2,3].

To date, these prior integrated demonstrations have been limited to operations using light of only a single linear polarization, specifically transverse electric (TE), nominally parallel to the ion-trap chip surface. However, diverse polarizations are critical for enabling many operations for advanced trapped-ion systems [4], leading to an interest in developing polarization-diverse emitters [5,6]. For example, integrated-photonics-based architectures involving light of both TE and transverse-magnetic (TM) polarizations (such as the configuration in Fig. 1a) are necessary for enabling advanced ion cooling schemes that offer sub-Doppler temperatures over several non-degenerate trap-vibrational modes, such as polarization-gradient and electromagnetically-induced-transparency cooling [4].

In this work, we design and experimentally demonstrate a pair of integrated TE- and TM-emitting gratings with an operating wavelength of 422 nm, corresponding to the $5^2S_{1/2}$ to $5^2P_{1/2}$ transition of $^{88}Sr^+$ ions, a key transition for ion control. We implement a custom optimization-based design algorithm to realize bilayer, apodized, and curved gratings that emit unidirectional focused beams, with experimentally measured spot dimensions of 7.6 μm × 4.3 μm for the TE grating and 5.0 μm × 3.6 μm for the TM grating at a target ion height of 50 μm above the surface of the chip. This work represents, to the best of our knowledge, the first development of integrated TM-emitting gratings for trapped-ion systems, and, thus, a fundamental stepping stone on the path to advanced operations for integrated-photonics-based trapped-ion quantum systems involving multiple polarizations.

2. Polarization-Diverse Grating Emitter Design Process and Simulation Results

Both of the gratings in this work are comprised of two 100-nm-thick layers of silicon nitride separated by 90 nm of silicon dioxide, with the grating teeth fully etched into the nitride. The pitch and duty cycles of each layer's grating teeth are optimized such that the gratings emit focused beam profiles that maximize the percentage of light emitted towards a target ion location 50 μm above the surface of the chip. In addition, the teeth in each layer are offset from each other in the propagation dimension (x) to enable unidirectional emission upwards [7]. Finally, the grating teeth are curved to enable focusing in the transverse dimension (y) of the grating.

To design each grating, we utilize a particle swarm algorithm to determine the optimal pitches, duty cycles, and offsets of the teeth in both layers. Then, we use a slab mode simulation to determine the optimal grating tooth curvature, based on the phase front of the mode propagating in the grating. Finally, we simulate the grating and compute its expected emission angle, beam dimensions, and efficiency.

The gratings developed in this work are designed with a 17 μm × 18 μm emitting aperture area. This size was chosen such that the optimized TE and TM gratings emit with matching efficiencies at the ion location – a necessary condition for many ion operations involving both polarizations, such as polarization-gradient cooling [4]. The resulting simulated emission profiles in the xz plane for both gratings are plotted in Fig. 1c-d. The TE grating has an expected emission angle of 48.6° and a spot size ($1/e^2$ diameter) of 9.9 μm × 5.0 μm at the ion location 50 μm above the chip surface. The TM grating has an expected emission angle of 47.8° and a spot size of 6.1 μm × 3.7 μm at the ion location 50 μm above the chip surface.

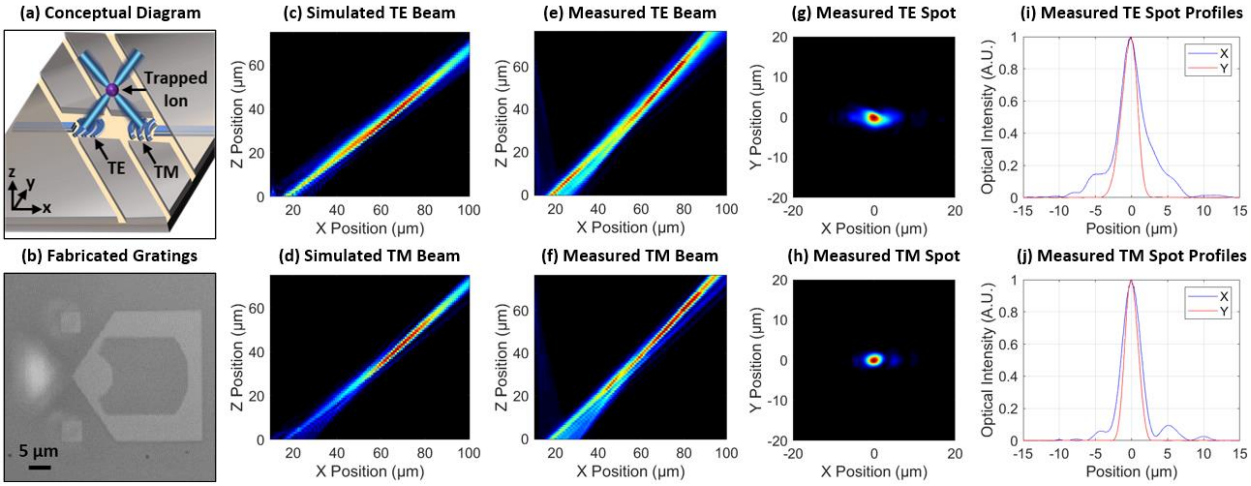

Fig. 1. (a) Conceptual diagram of an integrated trapped-ion addressing architecture, with two polarization-diverse gratings emitting focused beams towards a trapped ion (not to scale). (b) Micrograph of a fabricated grating. Simulated *xz* intensity profiles for the (c) TE and (d) TM grating. Experimentally measured *xz* intensity profiles for the (e) TE and (f) TM grating. Measured spots in the *xy* plane at $z = 50$ μm for the (g) TE and (h) TM grating. Measured spot profiles in the *x* (blue) and *y* (red) dimension at $z = 50$ μm for the (i) TE and (j) TM grating.

3. Polarization-Diverse Grating Emitter Fabrication and Experimental Results

The designed gratings were fabricated in our 200-mm wafer-scale fabrication process developed at MIT Lincoln Laboratory for wavelengths spanning the range from ultraviolet to near infrared (Fig. 1b) [8].

To characterize the gratings, light is routed from a benchtop laser to the chip through a series of polarization-maintaining fibers. To set the input polarization, we use a polarizing beam-splitter cube on a mount aligned with the axes of the chip to align the incident polarization of the fiber to the operating polarization of the grating under test (either TE or TM). We then remove the cube and couple the light onto the chip using an on-chip edge coupler. The light is then routed to the grating using a combination of alumina waveguides, silicon-nitride waveguides, and vertical layer transitions [8]. To measure each grating's performance, we visualize the chip with a 50X objective and a visible-light camera, and use an automated setup to increment the height of the optical train in 1-μm steps to capture images of the grating's emitted beam over a range of 0 to 100 μm above the surface of the chip (Fig. 1e-f). We then use the resulting data to compute the grating's emission angle and beam dimensions (Fig. 1g-j).

Using this characterization procedure, we find that the fabricated TE grating successfully emits TE-polarized light at an angle of 43.2° (Fig. 1e) with a spot size ($1/e^2$ diameter) of 7.6 μm × 4.3 μm at 50 μm above the chip surface (Fig. 1g). Similarly, the fabricated TM grating successfully emits TM-polarized light at an angle of 43.1° (Fig. 1f) with a spot size of 5.0 μm × 3.6 μm at 50 μm above the chip surface (Fig. 1h).

4. Conclusions and Acknowledgements

In this work, we designed and experimentally demonstrated a pair of integrated TE- and TM-emitting gratings with an operating wavelength of 422 nm, corresponding to the $5^2S_{1/2}$ to $5^2P_{1/2}$ transition of $^{88}Sr^+$ ions. This work represents, to the best of our knowledge, the first development of integrated TM-emitting gratings for trapped-ion systems, and, thus, a fundamental stepping stone on the path to advanced operations for trapped-ion quantum systems involving multiple polarizations, such as polarization-gradient and electromagnetically-induced-transparency cooling [4,9], using an integrated photonics platform.

This work was supported by the NSF QLCI HQAN (2016136), NSF QLCI Q-SEnSE (2016244), MIT CQE (H98230-19-C-0292), NSF GRFP (1122374), MIT Cronin Fellowship, and MIT Locher Fellowship.

5. References

[1] C.D. Bruzewicz et al., "Trapped-ion quantum computing: progress and challenges," Appl. Phys. Rev. **6**, 021314 (2019).
[2] R. Niffenegger *et al.*, "Integrated multi-wavelength control of an ion qubit," Nature **586**, 538–542 (2020).
[3] K. K. Mehta *et al.*, "Integrated optical multi-ion quantum logic," Nature **586**, 533–537 (2020).
[4] A. Hattori *et al.*, "Integrated-photonics-based architectures…," in Proceedings of Frontiers in Optics (FiO) (Optica, 2022), paper FM4B.3.
[5] L. Massai *et al.*, "Pure circularly polarized light emission from waveguide microring resonators," Appl. Phys. Lett. **121**, 121101 (2022).
[6] G. Spektor *et al.*, "Universal visible emitters in nanoscale integrated photonics," Optica **10**, 871-879 (2023).
[7] J. Notaros *et al.*, "Ultra-efficient CMOS…," in Proceedings of Optical Fiber Communication Conference (OFC) (Optica, 2016), paper M2I.5.
[8] C. Sorace-Agaskar *et al.*, "Versatile silicon nitride and alumina integrated…," IEEE J. Sel. Top. Quantum Electron. **25**(5), 1-15 (2019).
[9] T. Sneh *et al.*, "Design of integrated visible-light…," in Proceedings of Frontiers in Optics (FiO) (Optica, 2022), paper JTu5A.48.